


Cite this: *RSC Adv.*, 2021, **11**, 12802

Synthesis and characterization of new fluorescent boro- β -carboline dyes†

Dénes Szepesi Kovács,^{ab} Imre Hajdu,^{ab} Gergely Mészáros,^{cd} Lucia Wittner,^{id c} Domokos Meszéna,^{id cd} Estilla Zsófia Tóth,^{id ce} Zita Hegedűs,^f Ivan Randelović,^f József Tóvári,^f Tímea Szabó,^{id g} Bence Szilágyi,^b Mátyás Milen,^{id g} György Miklós Keserű^{id *ab} and Péter Ábrányi-Balogh^{id *ab}

The first representatives of the new fluorescent boro- β -carboline family were synthesized by the insertion of the difluoroboranyl group into the oxaza or diaza core. The resulting compounds showed good photophysical properties with fine Stokes-shifts in the range of 38–85 nm with blue and green emission. The energetics of the excitation states and molecular orbitals of two members were investigated by quantum chemical computations suggesting effects for the improved properties of diazaborinino-carbolines over oxazaborolo-carbolines. These properties nominated this chemotype as a new fluorophore for the development of fluorescent probes. As an example, diazaborinino-carbolines were used for the specific labeling of anti-Her2 antibody trastuzumab. The fluorescent conjugate showed a high fluorophore-antibody ratio and was confirmed as a useful tool for labeling and confocal microscopy imaging of tumour cells *in vitro* together with the *ex vivo* two-photon microscopy imaging of tumour slices.

Received 17th March 2021
Accepted 24th March 2021

DOI: 10.1039/d1ra02132j

rsc.li/rsc-advances

Introduction

Fluorophores or fluorescent probes are widely used tools in chemical biology for tagging proteins, cells or subcellular compartments in order to make the visualization of these species available. Although the development of synthetic fluorophores is important, Nature also gave us light absorbing and emitting tool compounds.^{1,2} A merged direction is the modification of natural compounds or their derivatives by turning them into efficient fluorophores. The β -carboline core is widely present in natural and synthetic biologically active compounds (Fig. 1).³ One of the most well-known families is represented by

the harmala alkaloids⁴ found in a high number of plants. Harmaline (1), its several tryptamine analogue derivatives (2) and other serotonin (3) receptor agonists show fluorescence properties.^{5,6} Particularly, β -carboline (4) and methyl- β -carboline-3-carboxylate (5) are responsible for the blue fluorescent cuticle of two scorpion species. The latter (5) and its 3,4-dihydro derivative (6) can also be found in the human grey cataract.⁷ In addition, as close relatives, melatonin (7) analogues equipped with a difluoroboranyl group (8) were identified as fluorescent melatonin receptor agonists,⁸ showing a structural similarity to the widely used BODIPY (9).⁹

In continuation of our research on new β -carboline derivatives^{10–13} and new fluorescent agents,¹⁴ we aimed to synthesize β -carbolines coordinating the BF₂ group either by two nitrogen atoms [like in BODIPY (9)] or a nitrogen and an oxygen [like boroisoquinolines(10)^{15,16}] (Fig. 1). Finding a possible application for this new family of fluorophores we aimed to equip them with functionalities to label antibodies for tumour diagnostics and to investigate the conjugates in confocal and two-photon microscopy (Fig. 1).^{14,17}

Results and discussion

After the successful synthesis of different boroisoquinolines^{15,16} we turned our attention to present a new fluorescent family based on the β -carboline core. Our design strategy was introducing the difluoroboranyl group between two heteroatoms (two nitrogens or a nitrogen and an oxygen) that was realized by the pyridoindeole structure containing two nitrogens in rings B and C. Thus, we

^aResearch Centre for Natural Sciences, Medicinal Chemistry Research Group, POB 286, 1519 Budapest, Hungary. E-mail: abrányi-balogh.peter@ttk.hu; keseru.gyorgy@ttk.hu; Tel: +36-13826961

^bDepartment of Organic Chemistry and Technology, Budapest University of Technology and Economics, 1521 Budapest, Hungary

^cResearch Centre for Natural Sciences, Comparative Psychophysiology Research Group, POB 286, 1519 Budapest, Hungary

^dFaculty of Information Technology and Bionics, Pázmány Péter Catholic University, POB 278, 1444 Budapest, Hungary

^eJános Szentágothai Doctoral School of Neurosciences, Semmelweis University, 1085, Budapest, Hungary

^fNational Institute of Oncology, Department of Experimental Pharmacology, POB 21, 1525 Budapest, Hungary

^gEgis Pharmaceuticals Plc., Directorate of Drug Substance Development, POB 100, 1475 Budapest, Hungary

† Electronic supplementary information (ESI) available: For experimental procedures and compound characterization. See DOI: 10.1039/d1ra02132j



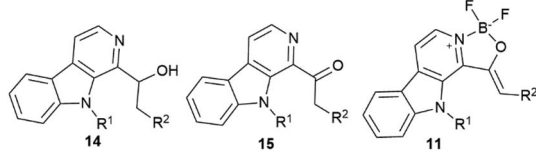
decided to synthesize members of two families, the oxazaborolo-carbolines (**11**) and the diazaborinino-carbolines (**12**) (Fig. 1).

Synthesis of oxazaborolo-carbolines (**11**)

For the synthesis of oxazaborolo-carbolines we used the natural product 1-formyl- β -carboline (**13**) (Kumujian C) synthesized in 5 steps using literature methods with good yields (61–95%), starting from tryptamine (**2**).²¹ Then Kumujian C has been transformed to 1-(ethyl-1-ol)- β -carbolines by Grignard reaction with methyl iodide, ethyl iodide, benzyl chloride and 4-methoxybenzyl-chloride resulting in **14a–d** with various yields (35–77%) (Table 1). The next step was the oxidation of **14** alcohols to ketones (**15**) using activated manganese(iv)-oxide (MnO_2) or Dess–Martin periodinane (DMP).

In some cases, MnO_2 led to significant degradation, but using DMP in milder conditions resulted in higher yields. Finally, we equipped the **15** keto- β -carbolines with the difluoroboranyl group using boron trifluoride diethyletherate in the presence of diisopropylethylamine (Scheme 1). These reactions showed good to excellent yields for the alkyl (methyl and ethyl,

Table 1 Results of the synthesis of 1-(ethyl-1-ol)- β -carbolines (**14**), **15** ketones and **11** boro- β -carbolines



| Entry | Compound | R ¹ | R ² | 14 [%] ^a | 15 [%] ^a | 11 [%] ^a |
|-------|----------|-----------------|-------------------------------------|----------------------------|----------------------------|----------------------------|
| 1 | a | H | H | 77 | 70 | 82 |
| 2 | b | H | CH ₃ | 66 | 57 | 55 |
| 3 | c | H | Ph | 73 | 46 | — |
| 4 | d | H | 4-MeO-C ₆ H ₄ | 35 | 52 | — |
| 5 | e | CH ₃ | H | 74 | 46 ^b | 79 |
| 6 | f | CH ₃ | CH ₃ | 72 | 50 ^b | 92 |

^a Isolated yields. ^b Yields with Dess–Martin periodinane.

15a and **15b**) ketones, but in the case of benzyl derivatives (benzyl and 4-methoxybenzyl, **15c** and **15d**) no product was detected by HPLC-MS. Under harsher conditions (higher equivalent of $\text{BF}_3 \cdot \text{OEt}_2$, reflux) still the starting material was recovered that can be explained by the electron withdrawing character of the aromatic moiety abolishing the reactivity of the nitrogen. Next, we planned to increase the electron density for better fluorescence by the introduction of an electron donating group to the nitrogen atom of the pyrrole ring. Kumujian C (**13**) was methylated with MeI in the presence of sodium hydride with good yield (76%). The next borylating step leading to **11e** and **11f** oxazaborolo-carbolines have been performed similar to **11a** and **11b** and led to the products in 79% and 92% yields, respectively (Table 1).

Synthesis of diazaborinino-carbolines (**12**)

The synthesis of diazaborinino-carbolines (**12**) started from tryptamine (**2a**) or tryptophan methyl ester (**2b**) (Scheme 2). In the case of **16a,b** the crude product of the first Pictet–Spengler reaction was taken directly to dehydrogenation (Method A). The β -carboline core was formed with moderate yields. In the case of **16c,d** the Pictet–Spengler reaction and the dehydrogenation was performed in one-pot reaction at 140 °C with a slightly longer reaction time, following the method of Singh *et al.* with modifications (Method B).²² Finally, the difluoroboranyl group was incorporated to the structure by $\text{BF}_3 \cdot \text{OEt}_2$ in the presence of Na_2CO_3 at 85 °C leading to the desired heterocycles in acceptable to high yields (up to 95%) (Table 2). Notably, the imidazole-derivative (**12a**) gave the lowest yield that could be rationalized by its instability due to the decreased donor effect of the smaller aromatic ring to the N–B bond formation. In the final step, it was crucial to work under dry conditions. The work-up could be performed by a simple filtration through celite followed by chromatography.

Photophysical properties

After the synthesis of the borocarbolines (**11a,b,e,f** and **12a–d**), we have investigated the absorption, excitation and emission

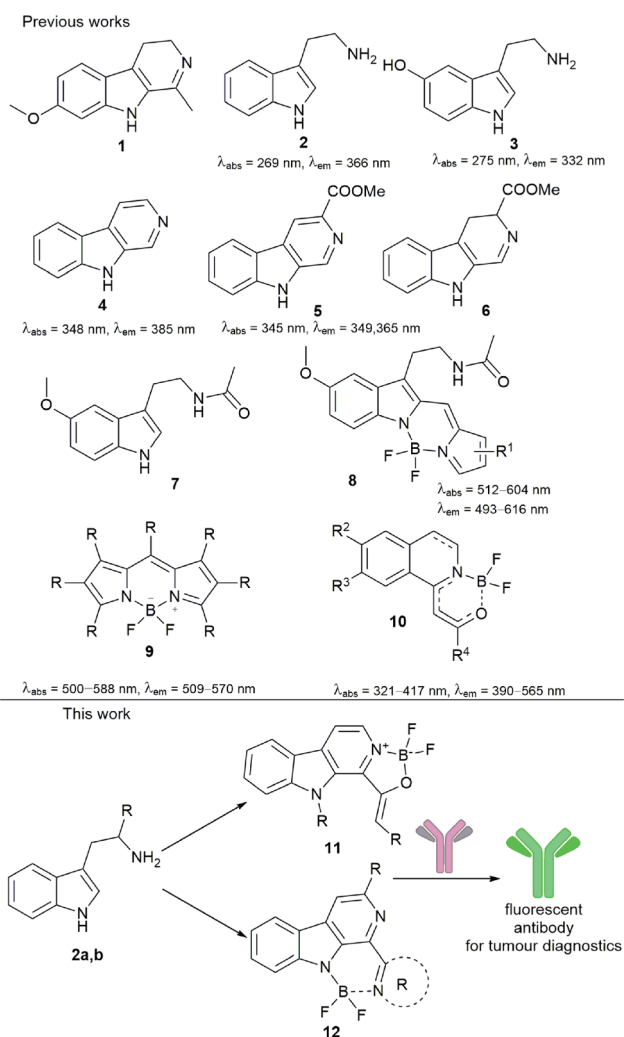
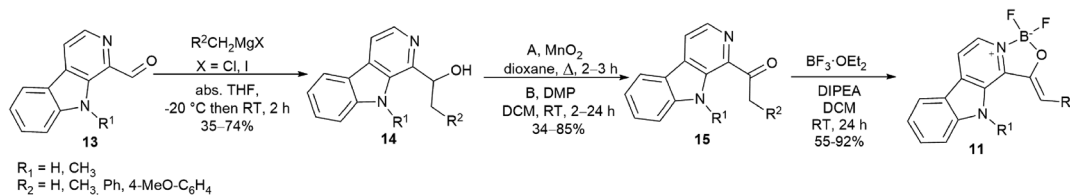
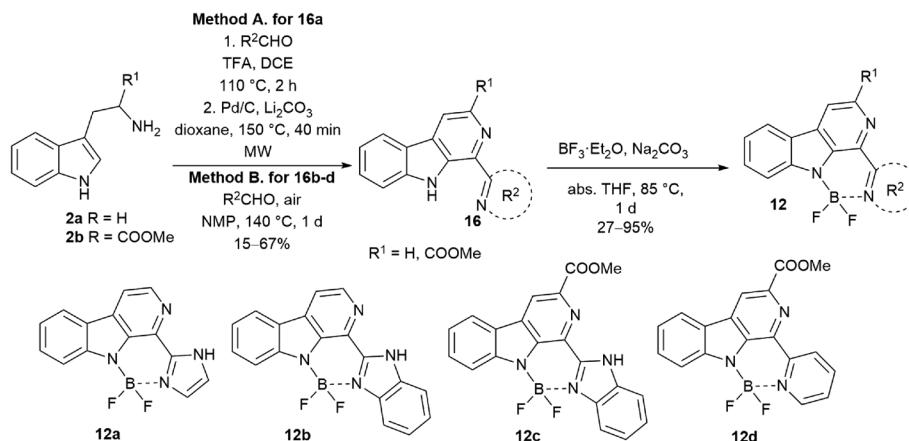


Fig. 1 Biologically active and fluorescent compounds together with the aims of this work.^{18–20}

Scheme 1 Synthesis of oxazaborolo-carbolines (**11**).Scheme 2 Synthesis of diazaborinino-carbolines (**12a-d**).

spectra, molar absorption coefficients, quantum yields and brightness. Specific wavelengths are given in Table 3. The absorbance maxima are usually located in the range of near UV (363–396 nm for compounds **11a,b,e,f** and **12a**), but three derivatives goes up to low-vis (405–414 nm for compounds **12b-d**). The emission maxima are found from blue light to the beginning of green light of the visible spectra (417–489 nm). The oxazaborolo-carbolines (**11a,b,e,f**) are shifted hypsochromic direction if we compare it with the diazaborinino-carbolines (**12a-d**). The Stokes shifts are usually in a range of 60 to 85 nm that can be considered as relatively large compared to the widely used BODIPY dyes (6–32 nm).

The molar absorbance coefficient is generally lower for oxazaborolo-carbolines than the diazaborinino carbolines, and the same phenomenon can be observed regarding the quantum yields resulting in usually moderate brightness values. Outstanding compound is **12d** borocarboline with good brightness ($B = 6360 \text{ M}^{-1} \text{ cm}^{-1}$) and the largest Stokes shift (85

nm). We hypothesize that the lower flexibility of the core and less enhanced push-pull system are behind the weaker photo-physical properties of oxazaborolo compounds.

Computed properties

The best members of each family were chosen for quantum chemical investigations. The optimal geometry conformers of compounds **11f** and **12d** were taken in S_0 and S_1 states, and transition energies were calculated. These calculations showed only small difference between the excitation and relaxation energy values (Fig. 2), just like in the energy of the band gap between the HOMO and LUMO orbitals (5.72 eV for **11f** and 5.48 eV for **12d**). The trends were the same, the less energy was in correspondence with the lower energy gap. Studying the change in the HOMO and LUMO energies upon excitation, it could be seen that for both compounds the LUMO level decreased similarly by 30–31 kJ mol^{-1} , while the HOMO increased by **11f** with 31.9 kJ mol^{-1} , and by **12d** with 16.1 kJ mol^{-1} . These data suggest that the better fluorescence properties of **12d** might be caused by the lower energy excited state, the lower HOMO–LUMO band gap and the lower excited state HOMO energy difference. Visualizing the molecular orbitals, many similar patterns could be observed between the HOMO and LUMO of **11f** and **12d** because of the common carboline core (Fig. 2). Interestingly, however, the participation of BF_2 in the HOMO was larger in the structure of **12d** while quite different conjugations could be observed in HOMO-1 orbital. This suggests that the vinylene group next to the oxazaborolidine ring has different effect than the

Table 2 Results of the synthesis of compounds **16a-d** and **12a-d**

| Entry | Compound | R^1 | R^2 | 16 [%] ^a | 12 [%] ^a |
|-------|----------|-------|------------------|----------------------------|----------------------------|
| 1 | a | H | Im ^b | 49 | 27 |
| 2 | b | H | Bim ^c | 33 ^c | 95 |
| 3 | c | COOMe | Bim ^c | 67 ^e | 63 |
| 4 | d | COOMe | Py ^d | 15 ^e | 74 |

^a Isolated yields. ^b Imidazole-2-yl. ^c Benzimidazole-2-yl. ^d Pyridine-2-yl.

^e Method B was applied.



Table 3 Photophysical properties of oxazaborolo- and diazaborinino carbolines

| # | Compound | R ₁ | R ₂ | $\lambda_{\text{abs}}^{\text{max}}$ [nm] | $\lambda_{\text{exc}}^{\text{max}}$ [nm] | $\lambda_{\text{em}}^{\text{max}}$ [nm] | $\Delta\lambda$ [nm] | ϵ ($\lambda_{\text{abs}}^{\text{max}}$) [M ⁻¹ cm ⁻¹] | Φ_F [-] | B [M ⁻¹ cm ⁻¹] |
|---|------------|----------------|------------------|--|--|---|----------------------|--|--------------|---------------------------------------|
| 1 | 11a | H | H | 375 | 378 | 450 | 75 | 506 | 0.49 | 248 |
| 2 | 11b | H | Me | 379 | 376 | 417 | 38 | 11 700 | 0.21 | 2460 |
| 3 | 11e | Me | H | 377 | 377 | 445 | 68 | 5150 | 0.0062 | 32 |
| 4 | 11f | Me | Me | 363 | 378 | 435 | 72 | 11 700 | 0.27 | 3160 |
| 5 | 12a | H | Im ^a | 396 | 380 | 472 | 76 | 3750 | 0.40 | 1500 |
| 6 | 12b | H | Bim ^b | 414 | 398 | 484 | 70 | 8860 | 0.45 | 3990 |
| 7 | 12c | COOMe | Bim ^b | 405 | 393 | 465 | 60 | 9320 | 0.47 | 4380 |
| 8 | 12d | COOMe | Py ^c | 407 | 404 | 489 | 85 | 23 500 | 0.27 | 6360 |

^a Imidazole-2-yl. ^b Benzimidazole-2-yl. ^c Pyridine-2-yl.

pyridine ring connected to the carboline core. The vinylene group participates in the highest occupied orbitals and it is more distant from the BF₂ group, while the pyridine is directly connected participating only in HOMO. The atomic charges and the electron density was also investigated (Fig. 2). The partial negative charges are lower around BF₂ of **12d**, the electron density is more homogenous than that for **11f**. In the latter the vinylene group acts as a borderline between the negatively and positively charged parts of **11f**.

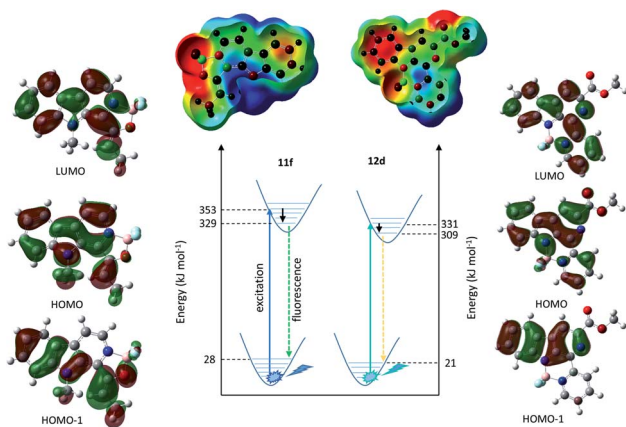


Fig. 2 Schematic representation of the excitation and fluorescence with computed energetics together with the visualized molecular orbitals, atomic charges and electrostatic potential (ESP) surface for **11f** and **12d**. On the ESP surface charges change from red (negative) to blue (positive). The atomic charges change from red (negative) to green (positive).

Effects of solvents and pH

Next, the performance of the best of each fluorescent carboline families (**11f** and **12d**) were investigated in different solvents. This solvent screen showed that the wavelength and intensity of emission of **11f** shifts in bathochromic direction with the increasing polarity of the solvent (e.g. in acetonitrile, EtOH or water, Fig. 3a). The intensity is the greatest in acetonitrile, but in water we still have decent emission, and the emission maximum is above 450 nm. In the case of **12d** the intensity decreased as we headed towards more polar solvents, but except of water the emission maximum did not change significantly (Fig. 3b). Notably, in water, the emission maxima shifted above 500 nm. The fluorescence of **12d** did not change significantly in the pH range of 4.4–8.4 (Fig. S9†).

Stability

Finally, to prove the ability for biological application, we have investigated the photostability of **11f** and **12d** in acetonitrile, excited with UV light (8 W, 366 nm). The half of the original fluorescence intensity was reached after 1 h irradiation by **11f**, but on the contrary, that did not decrease significantly after 1 h for **12d** (Fig. 4). We also followed the changes in 10% serum containing DMEM cell media and found **12d** stable over 24 hours (Fig. S10†). In addition, **12d** did not show cytotoxicity and neither anti-proliferative activity by the treatment of MRC-5 human lung fibroblast cell line for 24 h and 72 h, respectively (Tables S1 and S2, Fig. S11 and S12†).

These results show that both compounds are promising candidates for chemical biology applications, considering that the excitation during imaging procedures usually does not take more

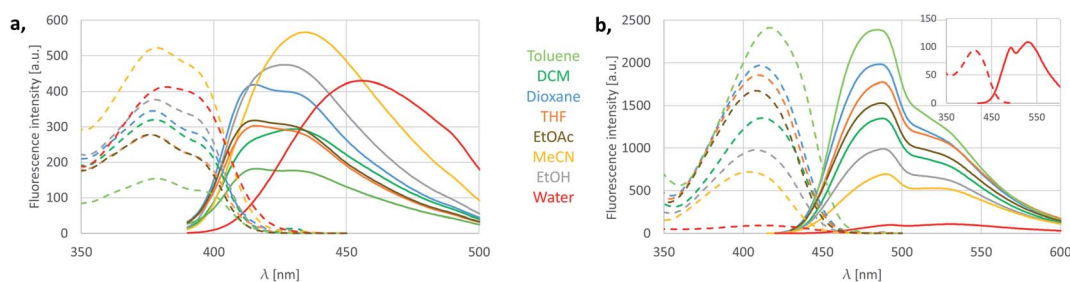


Fig. 3 Solvent effect on excitation and emission spectra of **11f** oxazaborolo-carboline (a) and **12d** diazaborinino-carboline (b).



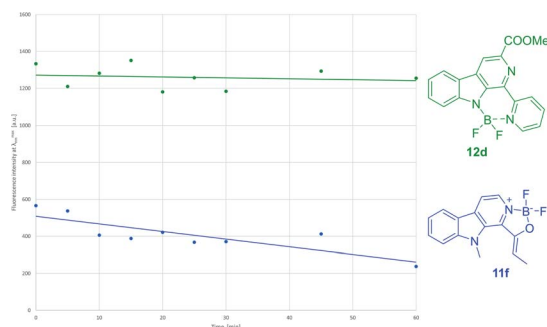


Fig. 4 Photostability of **11f** and **12d** carbolines.

than dozens of minutes. Due to its easy coupling and beneficial photophysical properties we selected **12d** diazaborinino-carboline for antibody labelling experiments. Since antibodies are target cancer cells selectively, and deliver their fluorescent²³ or cytotoxic payloads²⁴ specifically, we have conjugated **12d** to the human IgG trastuzumab creating a potential diagnostic tool for imaging Her2 positive tumour cells (Scheme 3a).²⁵

Synthesis and biological evaluation of trastuzumab conjugate **18**

We hydrolysed **16d** ester with sodium hydroxide, followed by the incorporation of the difluoroboranyl group. Then carboxylic acid **12e** was transformed to **12f** NHS ester. Reverse-phase chromatography was necessary for purification that decreased the isolated yields unexpectedly after full conversion. The NHS-ester (**12f**) was able to acylate the free lysines on the antibody (Scheme 3a) leading to a conjugate (**18**).²⁶ The conjugate was analysed by SDS-PAGE to confirm the attachment of the fluorophores (Scheme 3b), and the fluorophore-antibody ratio (FAR) was determined by UV-VIS absorbance measurement to be FAR = 18.

Having the antibody-dye conjugate in hand, three types of tumour cell lines were treated (Fig. 5A). The animals were anaesthetized, and the tumours were resected and fixed. The 100 μ m thick slices were treated with **18** for 24 h. No specific signal could be detected in cells of the epithelial human breast cancer cell line MDA-MB-231 negative for Her2 by confocal microscopy (Fig. 5A left). The cell membrane of the OVCAR-8, an ovarian carcinoma

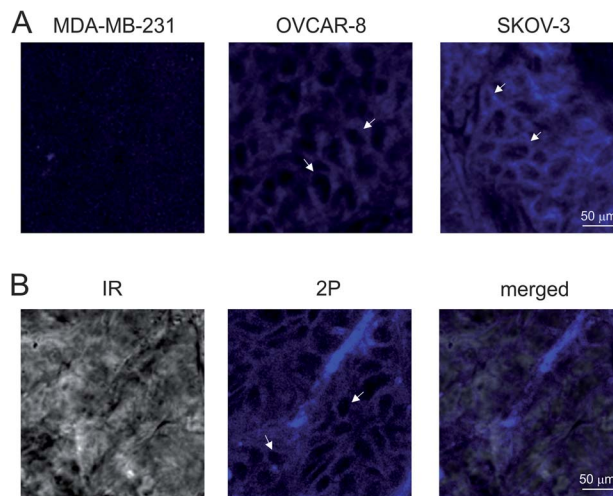
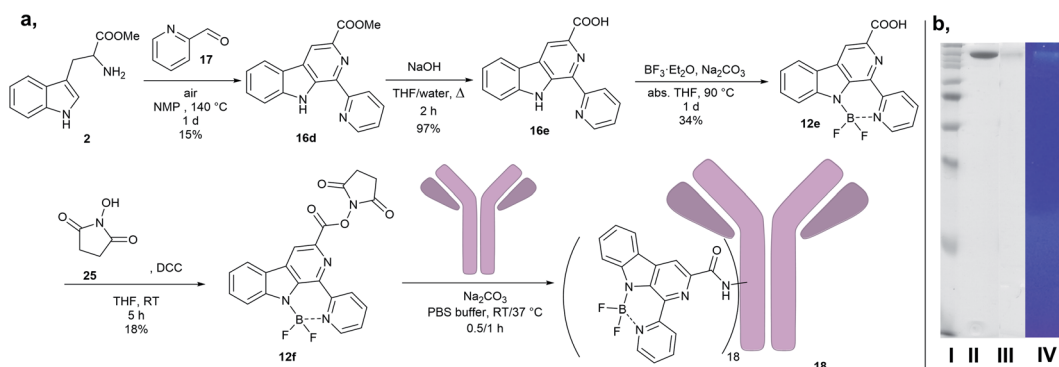


Fig. 5 (A) Confocal images showing the BK-bound trastuzumab antibody (**18**) on MDA-MB-231 (left), OVCAR-8 (middle) and SKOV-3 (right) tumour sections. Note that only the cell membrane is marked, therefore cells appear as circles (white arrows). Scale bar: 100 μ m. (B) Two-photon microscopy images of living tumour tissue incubated with the BK-bound trastuzumab antibody. Infrared image (IR, left) shows the tumour tissue, fluorescent image (middle) demonstrates that cells of the SKOV-3 tumours bound the antibody. Note that the fluorescent image is coloured artificially. Connective tissue surrounding the groups of tumour cells are autofluorescent. Scale bar: 50 μ m.

cell line slightly positive for Her2, tumour cells emitted a slight signal (Fig. 5A middle), whereas SKOV-3 an ovarian cell line expressing high amounts of Her2 showed a stronger signal (Fig. 5A right). For the two photon imaging tumours were resected from the anaesthetised animals, and 200 μ m thick slices were cut. The living tumour tissue was incubated with **18** at 35 $^{\circ}$ C for 1 h. The fluorescent image demonstrated that **18** antibody was bound to the cells of the SKOV-3 tumours (Fig. 5B).

Ethical statement

All animal experiments will be conducted following standards and procedures approved by the Animal Care and Use



Scheme 3 (a) Synthesis of **12f** dye with NHS ester group and antibody-fluorophore conjugate **18**; (b) SDS-PAGE in non-reducing gel: (I) molecular weight protein marker (kDa), (II) trastuzumab, (III) **18**, (IV) **18** under 366 nm light.



Committee of the National Institute of Oncology, Budapest (license number: PEI/001/2574-6/2015).

Conclusions

We have synthesized new families of boro- β -carbolines including oxazaborolo-carbolines and the diazaborinino-carbolines. Their photophysical analysis showed that the compounds can be excited in the 370–405 nm range, and emitting up to 489 nm. Stokes-shifts are greater than those of the BODIPY derivatives indicating their potential in chemical biology applications. Brightness data are acceptable and photostability was impressive by the best member of the diazaborinino-carbolines. The energetics of excitation states and molecular orbitals of two representatives were investigated by quantum chemical computations suggesting effects for the improved properties of diazaborinino-carbolines over oxazaborolo-carbolines. The best diazaborinino-carboline (**12d**) was further functionalized to an NHS-ester (**12f**) that was successfully used for antibody labelling and visualizing Her2 positive tumour cells in confocal and two-photon microscopy.

Conflicts of interest

There are no conflicts to declare.

Acknowledgements

Supported by the 2018-1.3.1-VKE-2018-00032 and Hungarian Thematic Excellence Programme TKP2020-NKA-26 grant of the National Office of Science, Innovation and Technology (NKFIH). We are grateful for the support of NKFIH PD124598 and ÚNKP-19-3-I-BME-408 New National Excellence Program of the Ministry for Innovation and Technology. The authors acknowledge the supportive work of Krisztina Németh.

Notes and references

- 1 A. J. Singh, A. P. Gorka, H. R. Bokesch, A. Wamiru, B. R. O'Keefe, M. J. Schnermann and K. R. Gustafson, *J. Nat. Prod.*, 2018, **81**, 2750–2755.
- 2 R. Duval and C. Duplais, *Nat. Prod. Rep.*, 2017, **34**, 161–193.
- 3 E. V. Costa, M. L. B. Pinheiro, C. M. Xavier, J. R. A. Silva, A. C. F. Amaral, A. D. L. Souza, A. Barison, F. R. Campos, A. G. Ferreira, G. M. C. Machado and L. L. P. Leon, *J. Nat. Prod.*, 2006, **69**, 292–294.
- 4 J. S. Glasby, *Encyclopedia of the Alkaloids*, Springer US, Boston, MA, 1983.
- 5 R. A. Glennon, M. Dukat, B. Grella, S.-S. Hong, L. Costantino, M. Teitler, C. Smith, C. Egan, K. Davis and M. V. Mattson, *Drug Alcohol Depend.*, 2000, **60**, 121–132.
- 6 J. Hidalgo, C. Carmona, M. Balón and M. A. Muñoz, *Pharm. Weekbl., Sci. Ed.*, 1990, **12**, 142–144.
- 7 S. J. Stachel, S. A. Stockwell and D. L. Van Vranken, *Chem. Biol.*, 1999, **6**, 531–539.
- 8 J. Thireau, J. Marteaux, P. Delagrange, F. Lefoulon, L. Dufourny, G. Guillaumet and F. Suzenet, *ACS Med. Chem. Lett.*, 2014, **5**, 158–161.
- 9 A. Loudet and K. Burgess, *Chem. Rev.*, 2007, **107**, 4891–4932.
- 10 M. Milen, P. Abranyi-Balogh, Z. Mucsi, A. Dancso, D. Frigyes, L. Pongo and G. Keglevich, *Curr. Org. Chem.*, 2013, **17**, 1894–1902.
- 11 M. Milen, P. Abranyi-Balogh, Z. Mucsi, A. Dancso, T. Kortvelyesi and G. Keglevich, *Curr. Org. Chem.*, 2011, **15**, 1811–1825.
- 12 P. Ábrányi-Balogh, T. Földesi, A. Grün, B. Volk, G. Keglevich and M. Milen, *Tetrahedron Lett.*, 2016, **57**, 1953–1957.
- 13 M. Milen, P. Slégel, P. Keglevich, G. Keglevich, G. Simig and B. Volk, *Tetrahedron Lett.*, 2015, **56**, 5697–5700.
- 14 L. Petri, P. A. Szijj, Á. Kelemen, T. Imre, Á. Gömöry, M. T. W. Lee, K. Hegedűs, P. Ábrányi-Balogh, V. Chudasama and G. M. Keserű, *RSC Adv.*, 2020, **10**, 14928–14936.
- 15 D. Sóvári, A. Kormos, O. Demeter, A. Dancsó, G. M. Keserű, M. Milen and P. Ábrányi-Balogh, *RSC Adv.*, 2018, **8**, 38598–38605.
- 16 D. Sóvári, G. M. Keserű and P. Ábrányi-Balogh, *Materials*, 2020, **13**, 199.
- 17 J. M. Warram, E. de Boer, A. G. Sorace, T. K. Chung, H. Kim, R. G. Pleijhuis, G. M. van Dam and E. L. Rosenthal, *Cancer Metastasis Rev.*, 2014, **33**, 809–822.
- 18 A. Chattopadhyay, R. Rukmini and S. Mukherjee, *Biophys. J.*, 1996, **71**, 1952–1960.
- 19 D. Reyman, M. J. Tapia, C. Carcedo and M. H. Viñas, *Biophys. Chem.*, 2003, **104**, 683–696.
- 20 A. Mallick, P. Das and N. Chattopadhyay, *J. Photochem. Photobiol., C*, 2010, **11**, 62–72.
- 21 T. Szabó, V. Hazai, B. Volk, G. Simig and M. Milen, *Tetrahedron Lett.*, 2019, **60**, 1471–1475.
- 22 V. Kumar, D. Singh, A. K. Paul, R. Shrivastava and V. Singh, *New J. Chem.*, 2019, **43**, 18304–18315.
- 23 J. M. Warram, E. de Boer, A. G. Sorace, T. K. Chung, H. Kim, R. G. Pleijhuis, G. M. van Dam and E. L. Rosenthal, *Cancer Metastasis Rev.*, 2014, **33**, 809–822.
- 24 P. Khongorzul, C. J. Ling, F. U. Khan, A. U. Ihsan and J. Zhang, *Mol. Cancer Res.*, 2020, **18**, 3–19.
- 25 T. A. D. Smith, *Br. J. Radiol.*, 2010, **83**, 638–644.
- 26 C. Martin, G. Brachet, C. Colas, E. Allard-Vannier, C. Kizlik-Masson, C. Esnault, R. Respaud, C. Denevault-Sabourin, I. Chourpa, V. Gouilleux-Gruart, M.-C. Viaud-Massuard and N. Joubert, *Pharmaceuticals*, 2019, **12**, 176.

